Received: 29 May 2022 | Revised: 16 October 2022 | Accepted: 25 October 2022

DOI: 10.1002/jnr.25142

RESEARCH ARTICLE

JOURNAL OF Neuroscience Research

Unruptured brain arteriovenous malformations causing seizures localize to one common brain network

Shao-Zhi Zhao[1,2] | Yu-Xin Zhao[3,4] | Xiao-Hua Liao[3,4] | Ran Huo[1,2] | Hao Li[1,2] | Yu-Ming Jiao[1,2] | Jian-Cong Weng[1,2] | Jie Wang[1,2] | Bing Liu[5,6] | Yong Cao[1,2]

[1]Department of Neurosurgery, Beijing Tiantan Hospital, Capital Medical University, Beijing, China

[2]China National Clinical Research Center for Neurological Diseases, Beijing, China

[3]Brainnetome Center and National Laboratory of Pattern Recognition, Institute of Automation, Chinese Academy of Sciences, Beijing, China

[4]School of Artificial Intelligence, University of Chinese Academy of Sciences, Beijing, China

[5]State Key Laboratory of Cognitive Neuroscience and Learning, Beijing Normal University, Beijing, China

[6]Chinese Institute for Brain Research, Beijing, China

Correspondence
Yong Cao, Department of Neurosurgery, Beijing Tiantan Hospital, Capital Medical University, 119 South Fourth Ring Road West, Fengtai District, Beijing 100070, China.
Email: caoyong@bjtth.org

Bing Liu, State Key Laboratory of Cognitive Neuroscience and Learning, Beijing Normal University, Beijing 100875, China.
Email: bing.liu@bnu.edu.cn

Funding information
National key research and development program of China during the 13th Five-Year Plan Period, Grant/Award Number: 2016YFC1301803

Abstract

Seizures are a frequent symptom of unruptured brain arteriovenous malformations (bAVMs). However, the brain regions responsible for these seizures remain unclear. To identify the brain regions causally involved in bAVM-related seizures, we retrospectively reviewed 220 patients with unruptured bAVMs. Using voxel-based lesion-symptom mapping (VLSM) analyses, we tested whether individual brain regions were associated with unruptured bAVM-related seizures. The result revealed that unruptured bAVMs causing seizures are anatomically heterogeneous at the voxel level. Subsequently, lesion network mapping (LNM) analyses was performed to determine whether bAVMs causing seizures belonged to a distributed brain network. LNM analyses indicated that these lesions were located in a functional network characterized by connectivity to the left caudate and precuneus. Moreover, the discrimination performance of the identified seizure network was evaluated in discovery set by calculating the individualized network damage score and was tested in validation set. Based on the calculated network damage scores, patients were divided into low-, medium-, and high-risk groups. The prevalence of seizures significantly differed among the three risk categories in both discovery ($p = .003$) and validation set ($p = .004$). Finally, we calculated the percentage of voxels in the canonical resting-state networks that overlapped with the seizure-susceptible brain regions to investigate the involvement of resting-state networks. With an involvement percentage over 50%, the frontoparietal control (82.9%), limbic function (76.7%), and default mode network (69.3%) were considered to be impacted in bAVM-related seizures. Our study identified the seizure-susceptible brain regions for unruptured bAVMs, which could be a plausible neuroimaging biomarker in predicting possible seizures.

KEYWORDS
brain arteriovenous malformations, lesion network mapping, seizures, voxel-based lesion-symptom mapping

Abbreviations: bAVMs, brain arteriovenous malformations; DMN, default mode network; DSA, digital subtraction angiography; FA, flip angle; FOV, field of view; FPN, frontoparietal control network; FWHM, full-width at half-maximum; GLM, general linear model; GRE-EPI, gradient-echo echo-planar imaging; LN, limbic network; LNM, lesion network mapping; MNI, Montreal Neurological Institute; ROI, region of interest; rs-fMRI, resting-state functional MR imaging; TE, echo time; TR, repetition time; VLSM, voxel-based lesion-symptom mapping.

Shao-Zhi Zhao, Yu-Xin Zhao, and Xiao-Hua Liao contributed equally to this work.

Edited by Cristina Antonella Ghiani and Elizabeth Johnson. Reviewed by James Christopher Mamaril-Davis and Shifu Li.

1 | INTRODUCTION

Brain arteriovenous malformations (bAVMs) are tangles of malformed vessels without capillary networks, and seizures are a frequent presenting symptom in patients with unruptured bAVMs (Hartmann & Mohr, 2015; Lawton et al., 2015). These seizures and the side effects of the antiepileptic drugs used to treat them profoundly impact patient quality of life. However, the underlying etiology of bAVM-induced seizures is not fully understood (Schramm, 2017). Previous studies implicated various characteristics, including lesion location, nidus size, venous congestion, and vascular steal phenomenon, as risk factors (Benson et al., 2020; Hoh et al., 2002; Schramm, 2017). Since seizures are considered a significant factor in the management of unruptured bAVMs to achieve a fully satisfactory outcome (Soldozy et al., 2020), a reliable risk prediction method for bAVM-related seizures is needed for clinical decision-making.

For unruptured bAVMs, previous studies have demonstrated that brain regions harbor differential seizure risks (Benson et al., 2020; Sun et al., 2016; Zhang et al., 2019). Meanwhile, seizures are considered a network disorder involving widespread structural alterations (Whelan et al., 2018). Although the brain regions associated with bAVM-related seizures have been anatomically identified at the brain region and subregion levels (Benson et al., 2020; Sun et al., 2016; Zhang et al., 2019), to date, neuronal dysfunction remote from the lesions has not been demonstrated in patients with unruptured bAVMs. In our study, we hypothesized that unruptured bAVMs causing seizures might anatomically map to individual brain regions and/or be located in the brain regions of a distributed brain network, which might be a potential neuroimaging biomarker for the prediction of bAVM-related seizures.

Recently, voxel-based lesion-symptom mapping (VLSM) and lesion network mapping (LNM) have been increasingly used to determine the relationships between brain lesions and clinical manifestations (Campanella et al., 2014; Corp et al., 2019; Darby et al., 2018; Wang et al., 2014). VLSM analyses can statistically assess the symptom-related brain regions on a voxel-by-voxel basis by overlapping lesion locations across patients with the same symptom (Bates et al., 2003). Using LNM analysis, lesions causing a variety of different neuropsychiatric symptoms can be mapped to functional brain networks by combining lesion locations with resting-state functional connectivity maps derived from healthy nonsymptomatic participants (Fox, 2018). With VLSM and LNM analyses, we can identify the neuroanatomical substrates associated with seizures and the seizure-susceptible brain regions within functional networks in patients with unruptured bAVMs.

In this study, we investigated the location of brain lesions in patients with unruptured bAVMs to identify the brain regions causally involved in seizure generation. Quantitative VLSM analysis was performed to assess the individual brain regions associated with bAVM-related seizures. Subsequently, we used LNM to test whether the lesions causing seizures were located within the brain regions of a functional network. The individualized network damage score was calculated to evaluate the performance of the identified seizure network in the prediction of bAVM-related seizures, and an external cohort was reviewed for validation. Finally, the percentage of the voxels in each of the seven canonical resting-state networks that overlapped with the brain regions for seizures was calculated to identify the canonical resting-state networks contributing to seizure generation in patients with unruptured bAVMs.

Significance

Seizures are a frequent symptom of unruptured brain arteriovenous malformations (bAVMs). These seizures and the side effects of the antiepileptic drugs used to treat them profoundly impact patient quality of life, making seizures a significant factor to be considered in the management of unruptured bAVMs. To achieve a fully satisfactory outcome, a reliable risk prediction method for bAVM-related seizures is needed for clinical decision-making. Our study indicated that unruptured bAVMs causing seizures, while anatomically heterogeneous, were located within a common network, which could be a plausible neuroimaging biomarker for the prediction of possible seizures.

2 | METHODS

2.1 | Patients

A total of 220 patients with unruptured bAVMs were retrospectively reviewed from Beijing Tiantan Hospital between May 2012 and June 2022. Patients included in this study met the following criteria: (1) patients with bAVMs were clinically diagnosed by neuroradiological data and unruptured bAVMs were defined based on the combination of medical history and radiological findings as previously reported (Fu et al., 2020); (2) patients underwent presurgical MRI; (3) detailed clinical records were available for the evaluation of seizures. Patients were ineligible if they met one or more of the following exclusion criteria: (1) patients with a history of surgical, endovascular, or stereotactic radiosurgical treatment for bAVMs; (2) patients with a history of other intracranial space-occupying lesions; and (3) available presurgical MRI with poor quality. Patients were divided into discovery and validation sets based on the available MRI data. One hundred and sixty-three patients with presurgical high-resolution structural images performed on a 3T magnetic resonance (MR) system (Siemens) with the same parameters were identified as a discovery set. Fifty-seven external patients whose presurgical structural images were acquired on 3T platforms (Siemens or GE) with various parameters were included in the validation set. This study was approved by the ethics committee of Beijing Tiantan Hospital, Capital Medical University, and written informed consent was obtained from all patients.

2.2 | Evaluation of bAVM-related seizures

The diagnosis of the seizure(s) was made according to the classification and terminology of the International League Against Epilepsy based on the patients' observed behavior (Fisher et al., 2017). Moreover, a patient was defined to have suffered from bAVM-related seizures when a history of at least one seizure in the presence of an enduring alteration in the brain (i.e., bAVM) was reported (Fisher et al., 2005).

2.3 | Brain imaging and lesion masking

High-resolution structural images of the discovery set (n = 163) were obtained on a 3.0-T MR system (Siemens). The acquired T1 anatomical image was a gradient-echo sequence: repetition time (TR) = 2300 ms, echo time (TE) = 2.98 ms, flip angle (FA) = 9°, field of view (FOV) = 256×256 mm^2, matrix = 64×64, voxel size = 1×1×1 mm^3, and slices = 176 (Jiao et al., 2019). T1 brain structure images in the validation set (n = 57) were acquired on GE or Siemens 3T platforms. The main protocol parameters were as follows: TR = 1750–2459 ms, TE = 8.6–19.9 ms, FA = 90–150°, FOV = 240×240 mm^2, matrix = 512×432–512×512, and slices = 23–24. The areas that produced abnormal hypointensive signals on T1 images were identified as lesion areas. Masks of lesions were drawn on each patient's T1-weighted image using ITK-SNAP software (v. 3.6.0, http://www.itksnap.org) by two neurosurgeons (Y.M.J. and H.L.) who were blinded to the patients' clinical information. Our inhouse python script based on the Python package nilearn (https://nilearn.github.io/stable/index.html) was applied to overlap the individual masks identified by the two neurosurgeons following lesion masking. We then calculated the percentage of the voxels in each lesion mask that did not overlap with the lesion mask identified by another neurosurgeon. If the percentage was less than 5%, the overlapped region was considered as the bAVM lesion and used for subsequent analyses. When the individual masks from the two neurosurgeons were inconsistent (>5%), the lesion mask we used was determined by a senior neurosurgeon (Y.C.). The T1 image and lesion mask for each patient were registered to the Montreal Neurological Institute (MNI) template using the standard nonlinear spatial normalization algorithm provided by FSL (https://fsl.fmrib.ox.ac.uk/).

2.4 | Voxel-based lesion-symptom mapping

To identify any brain voxels anatomically associated with seizures, VLSM analyses was applied in the discovery set (n = 163). VLSM is based on applying the general linear model (GLM) to each voxel independently (Bates et al., 2003). Specifically, the form of the generalized linear model is $Y = \beta X + \varepsilon$. The model parameter X represented the symptoms of the patients (1 indicated patients with seizures, and 0 indicated those without). For each voxel, Y represented lesion involvement in each patient (1 indicated that the voxel overlapped with the lesion, and 0 indicated that the voxel was outside the lesion). The model parameter β was estimated, and ε was the estimated residual. Finally, the p-value (voxelwise FDR-corrected $p < .05$) of the t-test for β indicated the sensitivity of the voxel to the seizure.

2.5 | Processing of normal resting-state functional MR imaging (rs-fMRI) dataset

To identify a common lesion network using the LNM method, we included a normal resting-state functional imaging dataset that included 358 healthy young Chinese subjects (183 males; mean age = 19.39±1.09 years; age range = 17.00–24.00 years; mean education years = 12.34±0.81 years). The dataset was acquired with a 3.0 T MR750 GE Scanner using a gradient-echo echo-planar imaging (GRE-EPI) sequence: TR = 2000 ms, TE = 30 ms, FA = 90°, FOV = 240×240 mm^2, matrix = 64×64, voxel size = 3.75×3.75×4 mm^3, and slices = 39. All the subjects were told to stay awake, close their eyes, and avoid movement during the scanning. More detailed data acquisition and preprocessing details can be found in our previous study (Liu et al., 2020).

Briefly, the following steps were applied: (1) removal of the first 10 timepoints and head motion correction; (2) rigid-body registration of the T1 image to the EPI mean image; (3) normalization of the EPI images to MNI standard space using the T1 image and subsequent resampling to 3×3×3 mm^3; (4) removal of noise, including the whole brain signals, head motions, and linear trends; (5) temporal filter (.01–.08 Hz); and (6) spatial smoothing using a 6-mm full-width at half-maximum (FWHM) isotropic Gaussian kernel.

2.6 | Lesion network mapping

To investigate the brain regions functionally connected to each lesion location in patients with bAVM-related seizures, we applied the validated technique termed lesion network mapping in the discovery set (Figure 1a). First, for patients with bAVM-related seizures, the registered lesions on the MNI template were used as a seed region to calculate the functional connectivity using resting-state fMRI data obtained from the 358 normal subjects mentioned above. The time series of all voxels within the lesions were averaged and correlated with the time series from all other brain voxels using Pearson's correlation coefficients. Fisher Z transform was used to ensure that the correlation coefficients were normally distributed. Second, for each patient, we derived network maps using a single sample t-test to combine across the 358 z-scores. Each network map was binarized at a T value of 0 (voxelwise FDR-corrected $p < .05$). Finally, to guarantee the consistence for the prevalence of the brain regions positively (0%–58.9%) and negatively (0%–81.1%) connected to the lesions in the healthy cohort, 50% was selected as the threshold to determine the brain regions sensitively connected with the lesion locations, which is consistent with the previous study on the

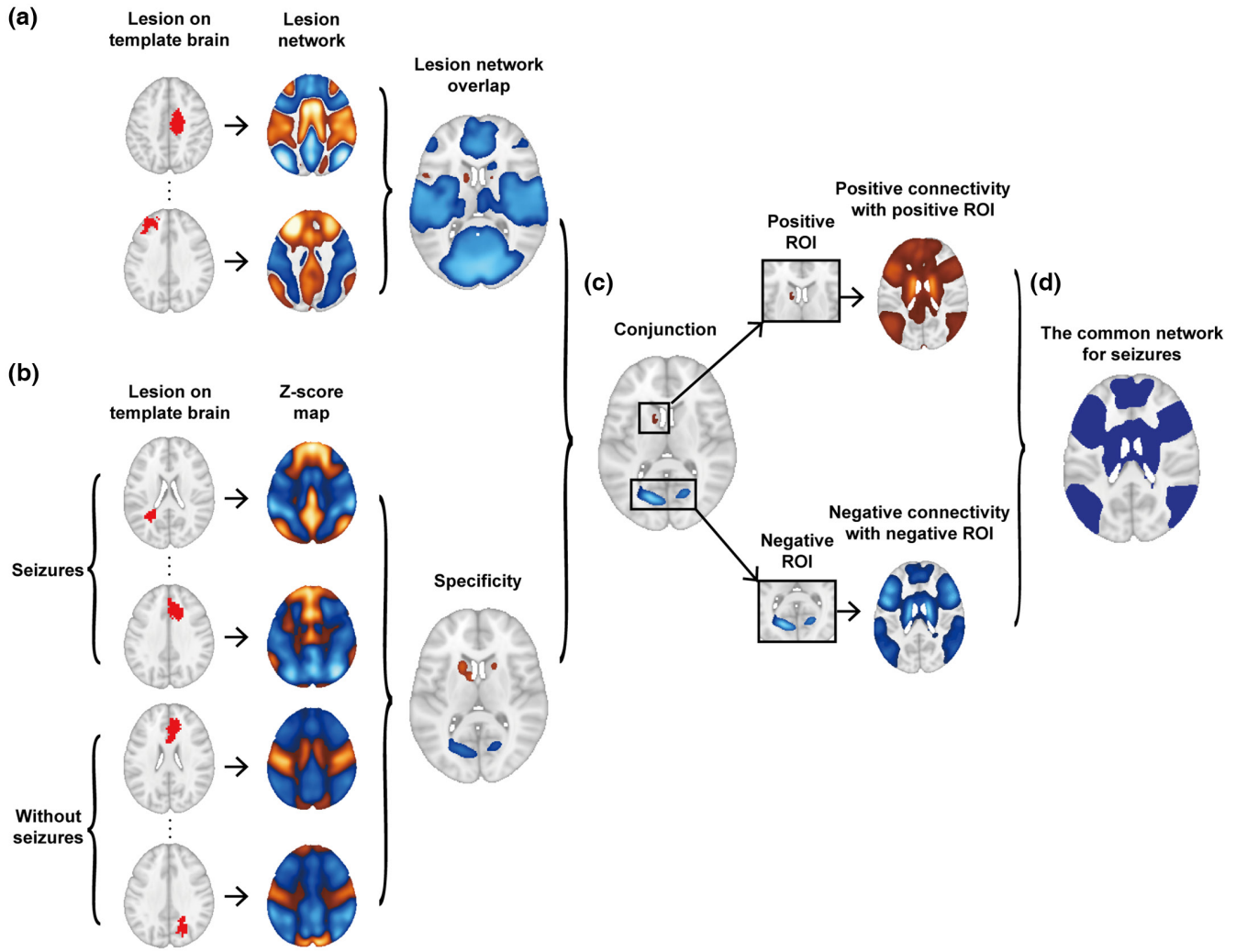

FIGURE 1 The workflow for identifying the bAVM-related seizure network. (a) Functional connectivity between each lesion location and the rest of the brain was computed using resting-state functional magnetic resonance imaging data from 358 healthy control subjects. Individual lesion network maps were thresholded, binarized, and overlapped to identify common connections across the lesion locations. (b) Specificity analyses was used to identify connections specific to patients with lesions causing seizures versus those without. (c) Conjunction analyses identified the regions of interest (ROIs) whose connectivity was both sensitive and specific to lesions causing seizures. (d) The overlap between the positive and negative connectivity patterns to the ROIs defining the set of brain regions in the seizure network.

brain network impaction of epileptogenic mass lesions (Mansouri et al., 2020). Specifically, the binarized lesion network maps were overlaid to identify voxels connected to more than 50% of the lesion locations associated with seizures. Moreover, we also conducted concordant analyses with the 40% threshold and found similar results (Figure S1).

2.7 | Specificity analyses

To evaluate the specificity of our findings, lesion network maps (average Fisher z values) were compared between patients with (n = 90) and without (n = 73) seizures (Figure 1b). Voxelwise two-sample t-tests were used to identify voxels significantly connected to lesions of the patients with seizures compared to those without using a voxelwise FDR-corrected $p < .05$.

2.8 | Conjunction analyses and seizure network definition

Conjunction analyses were performed to identify the brain regions both sensitively (voxels connected to >50% of lesion locations causing seizures) and specifically (voxels surviving specificity analyses) connected to the lesion locations in patients with bAVM-related seizures (Figure 1c). Conjunction analyses identified two regions of interest (ROIs): a positively correlated ROI in the left caudate and a negatively correlated ROI in the precuneus. By definition, connectivity with these two ROIs defines a distributed brain network that encompasses our lesion locations causing seizures (Figure 1d). To visualize this network, we identified voxels positively correlated with the left caudate ROI and voxels negatively correlated with the precuneus ROI. These two maps were then binarized and overlaid to identify the voxels meeting both criteria.

2.9 | Discrimination performance evaluation of the seizure network

To evaluate the performance of the seizure network in the prediction of bAVM-related seizures, we assigned each patient a "network damage score" by summing the intensity (t values) of the lesioned voxels that overlapped with the brain regions of the seizure network. Then, the mean network damage score among patients with lesions located in the seizure network was calculated and considered as the threshold for case classification. All subjects were then divided into three risk categories: the low-risk group (patients with lesions that did not overlap with the seizure network), the medium-risk group (patients with lesions that overlapped with the seizure network, but the network damage score did not exceed the threshold), and the high-risk group (patients with lesions that overlapped with the seizure network, and the network damage score exceeded the threshold). A Chi-square test was applied to evaluate whether the prevalence of seizures differed among the three risk categories. Moreover, an external cohort was reviewed to validate the discrimination performance of the seizure network.

2.10 | Overlap with canonical resting-state networks

The identified seizure-susceptible brain regions were overlapped with the seven canonical resting-state network atlas defined by Yeo et al. to assess the impact on resting-state networks in patients with bAVM-related seizures (Buckner et al., 2011). The percentage of voxels in each of the seven canonical resting-state networks that overlapped with the brain regions for seizures was calculated. When the percentage was over the threshold of 50%, abnormalities in the canonical resting-state network were considered to be associated with epileptogenesis in bAVM patients. Moreover, leveraging the spin-test MATLAB toolbox (Alexander-Bloch et al., 2018), we evaluated the significance of the overlap for each canonical resting-state network.

2.11 | Statistical analyses

2.11.1 | Demographic and clinical data

Statistical analyses of patients' demographic and clinical data were performed between patients with and without seizures and between patients in the discovery and validation sets. SPSS v22.0.0 (IBM, Armonk, New York) was used for statistical analyses in this part. Continuous variables are presented as means ± SD, and categorical variables are presented as numbers and percentages. Shapiro–Wilk test was applied to evaluate the normality of the continuous variables. For the data normally distributed, comparisons between two groups were performed by t-tests; otherwise, the Mann–Whitney test was applied. Chi-square tests were used for categorical variables. Statistical tests were considered significant at $p < .05$.

2.11.2 | Image data

The statistical analyses regarding the neuroimaging maps were conducted at the voxel-wise level using t-tests by the python package scipy (Virtanen et al., 2020), with the following multiple comparison correction implemented by python package statsmodels (Seabold & Perktold, 2010). Statistical tests were considered significant at voxelwise FDR-corrected $p < .05$.

2.11.3 | Evaluation of the identified seizure network

The difference in seizure prevalence was compared among the low-, medium- and high-risk groups in the discovery and the validation sets, respectively. A Chi-square test was performed via SPSS v22.0.0 (IBM, Armonk, New York) and was considered significant at $p < .05$.

3 | RESULTS

3.1 | Clinical characteristics

Between May 2012 and June 2022, a total of 220 patients with unruptured bAVMs were included in this study. Based on the collected neuroradiological data, patients were divided into a discovery set ($n = 163$) and a validation set ($n = 57$), with seizure prevalence rates of 55.2% and 47.4%, respectively. The clinical characteristics of patients with seizures, patients without seizures, the discovery set, and the validation set are listed in Table 1. Additionally, we listed the detailed demographics of the patients in Table S1. The ages of patients with ($n = 117$) or without ($n = 103$) seizures were 27.1 ± 12.5 years and 31.3 ± 12.6 years, respectively ($Z = -2.991$, $p = .003$). The lesion size of patients with seizures was 45.6 ± 12.5 mm and that of patients without seizures was 41.2 ± 11.7 mm ($t = -2.686$, $p = .008$). The clinical characteristics of the patients between the discovery set and the validation set were not significantly different.

3.2 | Locations of bAVMs causing seizures are heterogeneous

For patients in the discovery set, we generated lesion overlap maps to present an overview of the lesion distribution (Figure 2a–c). The maps display all voxels that were eligible for inclusion in the VLSM analyses, and the proportion of lesions overlapping on a single voxel was less than 12%. Comparing patients with ($n = 90$) and without

TABLE 1 Demographic and clinical characteristics of patients

Characteristics	Seizures $n = 117$	No seizures $n = 103$	Statistic	p Value	Discovery set $n = 163$	Validation set $n = 57$	Statistic	p Value
Age, (mean ± SD, years)	27.1 ± 12.5	31.3 ± 12.6	−2.991 †	.003¶,*	28.4 ± 12.0	31.0 ± 14.4	−1.067†	.286¶
Male, no. (%)	79 (67.5)	65 (63.1)	.472‡	.492‖	106 (65.0)	38 (66.7)	.050‡	.823‖
Size (mean ± SD, mm)	45.6 ± 12.5	41.2 ± 11.7	−2.686§	.008#,*	44.3 ± 12.6	41.3 ± 11.1	1.567§	.119#
Left side, no. (%)	58 (49.6)	58 (56.3)	.998‡	.318‖	87 (53.4)	29 (50.9)	.106‡	.745‖
Deep venous drainage, no. (%)	13 (11.1)	15 (14.6)	.588‡	.443‖	24 (14.7)	4 (7.0)	2.258‡	.133‖
S-M Grading, no. (%)			3.457‡	.494‖			6.882‡	.123‖
I	10 (8.5)	13 (12.6)			20 (12.3)	3 (5.3)		
II	47 (40.2)	46 (44.7)			62 (38.0)	31 (54.4)		
III	46 (39.3)	37 (35.9)			62 (38.0)	21 (36.8)		
IV	12 (10.3)	5 (4.9)			15 (9.2)	2 (3.5)		
V	2 (1.7)	2 (1.9)			4 (2.5)	0 (.0)		

Abbreviation: S-M Grading, Spetzler-Martin Grading.

Statistical value: †Z value; ‡χ^2 value; §T value.

Statistical test: ¶Mann–Whitney test; ‖Chi-square test; #t-test.

*$p < .05$.

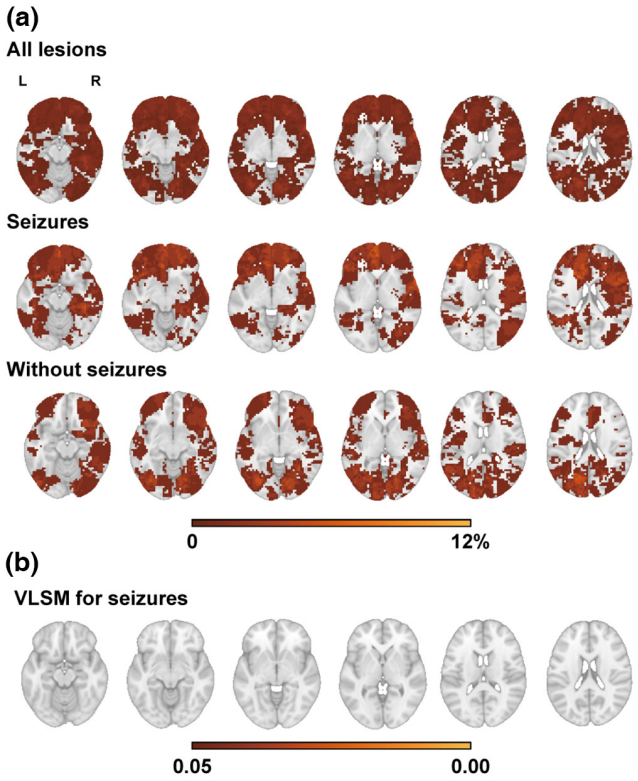

FIGURE 2 Lesion locations were not associated with seizures. (a) Lesion overlay map showing the percentage of patients among the three groups that overlapped in a particular voxel. Lighter colors indicate voxels where a larger proportion of patients had bAVMs. (b) Voxel lesion-symptom mapping (VLSM) identified no voxels significantly associated with seizures (FDR-adjusted $p < .05$).

($n = 73$) seizures, the VLSM analyses failed to identify any voxels significantly associated with seizures in the patients with unruptured bAVMs (Figure 2d).

3.3 | BAVM-causing seizures map to a common brain network

Despite the heterogeneity in lesion location, over 50% of lesion locations causing seizures exhibited positive connectivity with the superior frontal gyrus, middle frontal gyrus, inferior parietal lobule, inferior temporal gyrus, basal ganglia, etc., and negative functional connectivity with the medioventral occipital cortex, postcentral gyrus, lateral occipital cortex, precentral gyrus, and superior frontal gyrus, etc. (Figure 3a). Based on the specificity analyses, the pattern of lesion locations positively connected to the bilateral caudate and negatively connected to the precuneus was specific to bAVMs causing seizures compared to those without (Figure 3b). Finally, the conjunction analyses identified that connectivity to the left caudate and the precuneus was both sensitive and specific for bAVM-related seizures (Figure 3c). By definition, positive connectivity with the left caudate and negative connectivity with the precuneus defined the brain regions of the seizure network that tended to be epileptogenic (Figure 3d).

3.4 | Discrimination performance of the seizure network

The threshold utilized to divide the patients with lesions located in the seizure network into medium-risk and high-risk groups was 2779. In the discovery set, the percentages of patients with seizures in the low-, medium-, and high-risk groups were 31.8% (7/22), 51.1% (46/90), and 72.5% (37/51), respectively (Figure 4a). There was a significant difference in the prevalence of seizures among these three groups ($\chi^2 = 11.680$, $p = .003$). In the validation set, there were 10, 39, and 8 patients in the low-, medium-, and high-risk groups, respectively (Figure 4b). Moreover, a significant difference in the

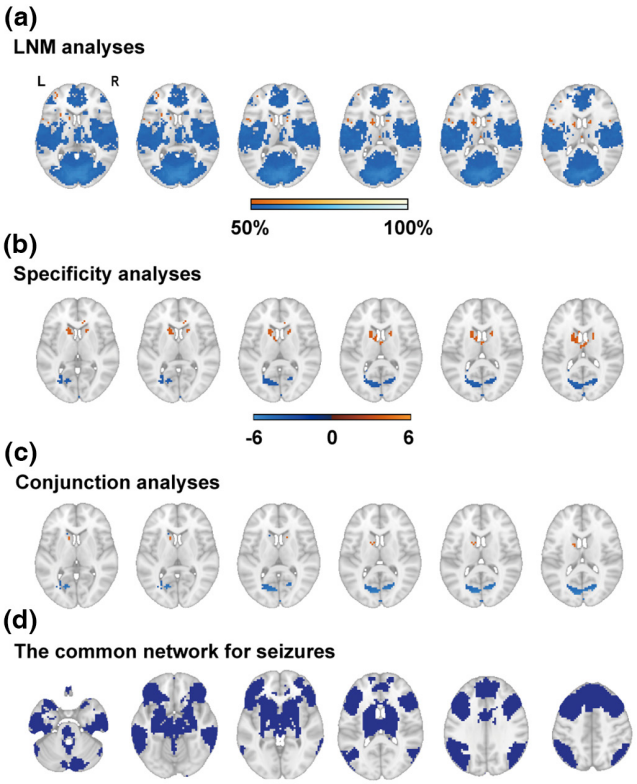

FIGURE 3 BAVMs causing seizures mapped to a common brain network. (a) LNM analyses indicated that lesion locations causing seizures were positively (red) correlated with the superior frontal gyrus, middle frontal gyrus, inferior parietal lobule, inferior temporal gyrus, basal ganglia, etc., and negatively (blue) correlated with the medioventral occipital cortex, postcentral gyrus, lateral occipital cortex, precentral gyrus, superior frontal gyrus, etc. Lighter colors indicate voxels where a larger proportion of individual lesion networks overlapped. (b) Positive connectivity to the bilateral caudate and negative connectivity to the precuneus were specific to patients with bAVM-related seizures compared to patients without seizures. (c) The conjunction analyses indicated that connectivity (positive in red and negative in blue) to the left caudate and the precuneus was both sensitive and specific for lesions causing seizures. (d) The overlap in brain regions negatively connected to the precuneus and positively connected to the left caudate defined the brain regions of the seizure network.

prevalence of seizures was identified among these three groups (10.0% vs. 48.7% vs. 87.5%, $\chi^2 = 10.783$, $p = .004$). Overlap between the regions of the seizure network and the lesions selected from the validation set is shown in Figure 4c, and we found that lesions in the patients with seizures were mostly located in the seizure network we defined.

3.5 | Canonical resting-state networks impacted in patients with unruptured bAVM-related seizures

The percentage of the voxels in each of the seven canonical resting-state networks that overlapped with the seizure network identified in patients with unruptured bAVMs is listed in Table 2. The canonical resting-state networks considered to be impacted in patients with unruptured bAVM-related seizures, determined by the overlap percentage that was over the threshold of 50%, were the frontoparietal control network (FPN) (82.9%), limbic network (LN) (76.7%), and default mode network (DMN) (69.3%). Moreover, leveraging the permutation test implemented in the spin-test toolbox (Alexander-Bloch et al., 2018), we also evaluated the significance of the overlap for each canonical resting-state network. The result (Table 2) indicated that the seizure network was significantly overlapped with the frontoparietal control network ($p < .001$) and default mode network ($p = .008$), and tended to be significantly overlapped with the limbic network ($p = .076$).

4 | DISCUSSION

In this study, we demonstrated that unruptured bAVMs causing seizures, despite being heterogeneous in their anatomical localization, were located in brain regions of a functional network. Specifically, these seizure-susceptible brain regions were functionally connected to the precuneus and the left caudate. This finding has potential implications for understanding the pathophysiology of bAVM-related seizures and assisting clinicians with personalized therapeutic decisions.

In the present study, we failed to find significant associations between bAVM locations and seizures using VLSM. We attribute this result to the heterogeneity in lesion location at the voxel level (Snider et al., 2020). Among the patients with and without seizures, the maximal proportion of lesions that overlapped on a single voxel was only 7% and 11%, respectively. Different from VLSM, which looks for associations with individual brain regions, LNM looks for associations with a distributed brain network (Fox, 2018). Using LNM, we identified that the unruptured bAVMs causing seizures were located in a functional network, which is consistent with the concept that seizures are network disorders involving widespread structural alterations.

In the current study, we identified that bAVMs causing seizures were connected to specific brain structures, including the left caudate and the precuneus. Abnormalities in these brain regions have been identified by other studies in connection to seizures. Structural changes in the caudate nucleus, including the loss of volume and increase in water diffusion, have been reported in seizures, suggesting the critical role of this structure within a broader epilepsy network (Luo et al., 2011; Riley et al., 2011). As a key hub of the DMN, the precuneus showed decreased cerebral blood flow in patients with seizures (Danielson et al., 2011; Nelissen et al., 2006).

The brain regions that functionally connect to the left caudate and the precuneus define a distributed functional brain network that encompasses lesions most likely to cause bAVM-related seizures. The overlap between these regions and the canonical resting-state networks revealed that the LN, the DMN, and the FPN were impacted in patients with unruptured bAVM-related

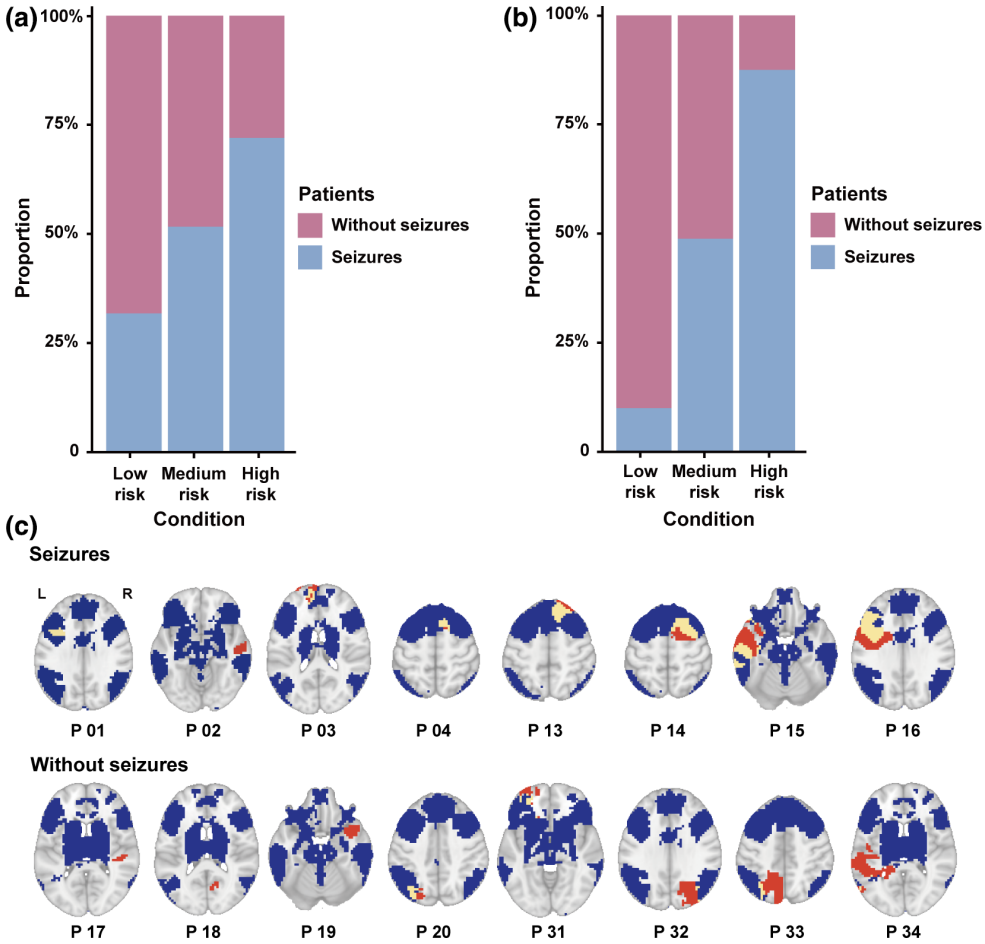

FIGURE 4 Validation of the seizure network. (a) In the discovery set, the percentages of patients with seizures in the low-, medium-, and high-risk groups were 31.8% (7/22), 51.1% (46/90), and 72.5% (37/51), respectively. A significant difference was identified among the three groups based on the Chi-square test ($\chi^2 = 11.680$, $p = .003$). (b) In the validation set, the percentages of patients with seizures in the low-, medium-, and high-risk groups were 10.0% (1/10), 48.7% (19/39), and 87.5% (7/8), respectively. A significant difference was validated among the three groups ($\chi^2 = 10.783$, $p = .004$). (c) Overlap (yellow) between the regions in the seizure network (blue) and the lesions selected from the validation set (red). The patients with and without seizures were sorted by lesion size. The four patients with the smallest lesions and the four with the largest lesions among the patients with and without seizures were selected for illustrative purposes.

TABLE 2 Overlap percentage between the common network for seizures and seven canonical resting-state networks

Network	Overlap percentage (%)	*p* Value
Frontoparietal control	82.9	<.001*
Limbic	76.7	.076
Default model	69.3	.008*
Salience / ventral attention	42.8	.462
Dorsal attention	38.4	.580
Visual	6.6	.961
Somatomotor	1.7	1.000

*$p < .05$.

seizures, suggesting that the FPN, LN, and DMN might be epileptogenic in patients with unruptured bAVMs. Previous studies have indicated the significance of LN, DMN, and FPN in epileptogenesis. The areas within the LN play a key role in epilepsy relying on their ability to produce and propagate synchronized physiological activity (He et al., 2017; Jo et al., 2019; Jobst & Cascino, 2017; Whelan et al., 2018). Additionally, the interconnection of LN structures through thalamic nuclei (part of the LN) has been a target for stimulation in the management of epilepsy (Khambhati et al., 2015). The DMN, representing a baseline state of the human brain that is associated with spontaneous activities such as mind wandering and consciousness maintenance, has been extensively explored in different neuropsychiatric patients (Brown et al., 2018; Mohan et al., 2016). Previous studies identified consistent cerebral blood flow changes in the structures of the DMN during seizures (Blumenfeld et al., 2004, 2009). Serving as a global functional hub, the FPN has broad connections with various brain networks (Elias et al., 2020). Altered intranetwork functional connectivity of the FPN has been demonstrated in patients with seizures (Wei et al., 2015).

In this study, patients were divided into low-, medium-, and high-risk groups based on the calculated network damage scores. The prevalence of seizures was significantly different among the three risk categories in both the discovery and validation sets, indicating favorable predictive efficacy of the seizure network with regard to bAVM-related seizures, which could be considered as a potential neuroimaging biomarker for the prediction of bAVM-related seizures. For patients with a low risk of seizures, conservative management with routine and periodic follow-up is recommended. However, intensive surveillance should be performed for those harboring bAVMs with a high probability of causing seizures. Additionally, considering that seizures are often unpredictable (Thurman et al., 2011), it is necessary for clinicians to remind patients with a high risk of seizures to strike a balance between their own quality of life and personal and public safety, including restricting driving, participating in sports with selection and direct supervision, and avoiding being solitary (Capovilla et al., 2016; Chen et al., 2014; Howard et al., 2004; Kang & Mintzer, 2016). This study is of great clinical significance considering that the identified seizure-susceptible brain regions within this seizure network might be a neuroimaging biomarker for the prediction of bAVM-related seizures. Based on the seizure-susceptible brain regions identified by LNM, a seizure risk evaluation software could be developed and attached to the hospital system in the future, with which clinicians can conveniently assess the risk of seizures by tracing the bAVMs on patients' neuroimaging data.

There are several limitations in the current study. First, the diagnosis of bAVM-related seizures was based on clinical presentation because the electroencephalographic data were unavailable. Second, its retrospective nature may make it difficult to avoid selection bias, information bias, and confounding factors. Third, given that the current study focused only on lesion location and connectivity to explain bAVM-related seizures, the dynamic compensatory mechanisms that unfold after a lesion occurs and the differences in patient age and lesion size between patients with and without seizures were not taken into consideration. Fourth, the separation between patients with and without seizures was based on whether the patients had a history of seizures, which has been widely used in previous studies (Liu et al., 2018; Wang et al., 2015; Zhang et al., 2019). Although some patients without seizures might suffer from seizures over time, we thought that the majority of those patients could be identified by the corresponding changes in neuroradiological data (i.e., enlargement or hemorrhage of lesions). Fifth, in our present study, the age ranges of patients were not limited. There may be differences in the brain regions between children and adults. Although the MNI template was applied to mitigate the impact of the difference in patient brain regions, future studies in patient groups of specific age range are warranted. Sixth, we divided patients into discovery and validation sets based on the available MRI data rather than randomly, which may influence the evaluation of the identified seizure network. Finally, the study only identified the brain regions associated with seizures in patients with unruptured bAVMs, and further work is needed to determine the difference among different seizure subtypes.

5 | CONCLUSION

Despite the absence of significant anatomical overlap among lesions causing seizures, unruptured bAVMs causing seizures were located within a functional network characterized by positive connectivity to the left caudate and negative connectivity to the precuneus, which may be a potential neuroimaging biomarker for the prediction of possible seizures in patients with unruptured bAVMs.

DECLARATION OF TRANSPARENCY

The authors, reviewers and editors affirm that in accordance to the policies set by the *Journal of Neuroscience Research*, this manuscript presents an accurate and transparent account of the study being reported and that all critical details describing the methods and results are present.

AUTHOR CONTRIBUTIONS

Conceptualization, S.-Z. Z., Y.-X. Z., and X.-H. L.; *Investigation*, S.-Z. Z., R. H., H. L., Y.-M. J., J.-C. W., and J. W.; *Data Curation*, S.-Z. Z., Y.-X. Z., and X.-H. L.; *Writing – Original Draft*, S.-Z. Z., Y.-X. Z., and X.-H. L.; *Writing – Review & Editing*, R. H., H. L., Y.-M. J., J.-C. W., B. L., and Y. C.; *Supervision*, B. L., and Y. C.; Project *Administration*, B. L., and Y. C.

ACKNOWLEDGMENT

We are grateful to Yi Zhai and Yue-Song Pan (China National Clinical Research Center for Neurological Diseases) for their advice in statistical assistance.

FUNDING INFORMATION

This study was supported by the "National key research and development program of China during the 13th Five-Year Plan Period" (Grant No. 2016YFC1301803, Principle Investigator: Professor Yong Cao).

CONFLICT OF INTEREST

The authors declare no conflict of interest.

PEER REVIEW

The peer review history for this article is available at https://publons.com/publon/10.1002/jnr.25142.

DATA AVAILABILITY STATEMENT

The data that support the findings of this study are available from the corresponding author upon reasonable request.

ORCID

Bing Liu https://orcid.org/0000-0003-2029-5187
Yong Cao https://orcid.org/0000-0002-8289-1120

REFERENCES

Alexander-Bloch, A. F., Shou, H., Liu, S., Satterthwaite, T. D., Glahn, D. C., Shinohara, R. T., Vandekar, S. N., & Raznahan, A. (2018). On

testing for spatial correspondence between maps of human brain structure and function. *NeuroImage*, *178*, 540–551. https://doi.org/10.1016/j.neuroimage.2018.05.070

Bates, E., Wilson, S. M., Saygin, A. P., Dick, F., Sereno, M. I., Knight, R. T., & Dronkers, N. F. (2003). Voxel-based lesion-symptom mapping. *Nature Neuroscience*, *6*(5), 448–450. https://doi.org/10.1038/nn1050

Benson, J. C., Chiu, S., Flemming, K., Nasr, D. M., Lanzino, G., & Brinjikji, W. (2020). MR characteristics of unruptured intracranial arteriovenous malformations associated with seizure as initial clinical presentation. *Journal of NeuroInterventional Surgery*, *12*(2), 186–191. https://doi.org/10.1136/neurintsurg-2019-015021

Blumenfeld, H., McNally, K. A., Vanderhill, S. D., Paige, A. L., Chung, R., Davis, K., Norden, A. D., Stokking, R., Studholme, C., Novotny, E. J., Jr., Zubal, I. G., & Spencer, S. S. (2004). Positive and negative network correlations in temporal lobe epilepsy. *Cerebral Cortex*, *14*(8), 892–902. https://doi.org/10.1093/cercor/bhh048

Blumenfeld, H., Varghese, G. I., Purcaro, M. J., Motelow, J. E., Enev, M., McNally, K. A., Levin, A. R., Hirsch, L. J., Tikofsky, R., Zubal, I. G., Paige, A. L., & Spencer, S. S. (2009). Cortical and subcortical networks in human secondarily generalized tonic-clonic seizures. *Brain*, *132*(Pt 4), 999–1012. https://doi.org/10.1093/brain/awp028

Brown, C. A., Jiang, Y., Smith, C. D., & Gold, B. T. (2018). Age and Alzheimer's pathology disrupt default mode network functioning via alterations in white matter microstructure but not hyperintensities. *Cortex*, *104*, 58–74. https://doi.org/10.1016/j.cortex.2018.04.006

Buckner, R. L., Krienen, F. M., Castellanos, A., Diaz, J. C., & Yeo, B. T. (2011). The organization of the human cerebellum estimated by intrinsic functional connectivity. *Journal of Neurophysiology*, *106*(5), 2322–2345. https://doi.org/10.1152/jn.00339.2011

Campanella, F., Shallice, T., Ius, T., Fabbro, F., & Skrap, M. (2014). Impact of brain tumour location on emotion and personality: A voxel-based lesion-symptom mapping study on mentalization processes. *Brain*, *137*(Pt 9), 2532–2545. https://doi.org/10.1093/brain/awu183

Capovilla, G., Kaufman, K. R., Perucca, E., Moshe, S. L., & Arida, R. M. (2016). Epilepsy, seizures, physical exercise, and sports: A report from the ILAE Task Force on Sports and Epilepsy. *Epilepsia*, *57*(1), 6–12. https://doi.org/10.1111/epi.13261

Chen, J., Yan, B., Lu, H., Ren, J., Zou, X., Xiao, F., Hong, Z., & Zhou, D. (2014). Driving among patients with epilepsy in West China. *Epilepsy & Behavior*, *33*, 1–6. https://doi.org/10.1016/j.yebeh.2014.01.020

Corp, D. T., Joutsa, J., Darby, R. R., Delnooz, C. C. S., van de Warrenburg, B. P. C., Cooke, D., Prudente, C. N., Ren, J., Reich, M. M., Batla, A., Bhatia, K. P., Jinnah, H. A., Liu, H., & Fox, M. D. (2019). Network localization of cervical dystonia based on causal brain lesions. *Brain*, *142*(6), 1660–1674. https://doi.org/10.1093/brain/awz112

Danielson, N. B., Guo, J. N., & Blumenfeld, H. (2011). The default mode network and altered consciousness in epilepsy. *Behavioural Neurology*, *24*(1), 55–65. https://doi.org/10.3233/ben-2011-0310

Darby, R. R., Horn, A., Cushman, F., & Fox, M. D. (2018). Lesion network localization of criminal behavior. *Proceedings of the National Academy of Sciences of the United States of America*, *115*(3), 601–606. https://doi.org/10.1073/pnas.1706587115

Elias, G. J. B., Giacobbe, P., Boutet, A., Germann, J., Beyn, M. E., Gramer, R. M., Pancholi, A., Joel, S. E., & Lozano, A. M. (2020). Probing the circuitry of panic with deep brain stimulation: Connectomic analysis and review of the literature. *Brain Stimulation*, *13*(1), 10–14. https://doi.org/10.1016/j.brs.2019.09.010

Fisher, R. S., Cross, J. H., French, J. A., Higurashi, N., Hirsch, E., Jansen, F. E., Lagae, L., Moshé, S. L., Peltola, J., Roulet Perez, E., Scheffer, I. E., & Zuberi, S. M. (2017). Operational classification of seizure types by the International League Against Epilepsy: Position Paper of the ILAE Commission for Classification and Terminology. *Epilepsia*, *58*(4), 522–530. https://doi.org/10.1111/epi.13670

Fisher, R. S., van Emde Boas, W., Blume, W., Elger, C., Genton, P., Lee, P., & Engel, J., Jr. (2005). Epileptic seizures and epilepsy: Definitions proposed by the International League Against Epilepsy (ILAE) and the International Bureau for Epilepsy (IBE). *Epilepsia*, *46*(4), 470–472. https://doi.org/10.1111/j.0013-9580.2005.66104.x

Fox, M. D. (2018). Mapping symptoms to brain networks with the human connectome. *The New England Journal of Medicine*, *379*(23), 2237–2245. https://doi.org/10.1056/NEJMra1706158

Fu, W., Huo, R., Yan, Z., Xu, H., Li, H., Jiao, Y., Wang, L., Weng, J., Wang, J., Wang, S., Cao, Y., & Zhao, J. (2020). Mesenchymal behavior of the endothelium promoted by SMAD6 downregulation is associated with brain arteriovenous malformation microhemorrhage. *Stroke*, *51*(7), 2197–2207. https://doi.org/10.1161/STROKEAHA.120.030046

Hartmann, A., & Mohr, J. P. (2015). Acute management of brain arteriovenous malformations. *Current Treatment Options in Neurology*, *17*(5), 346. https://doi.org/10.1007/s11940-015-0346-5

He, X., Doucet, G. E., Pustina, D., Sperling, M. R., Sharan, A. D., & Tracy, J. I. (2017). Presurgical thalamic "hubness" predicts surgical outcome in temporal lobe epilepsy. *Neurology*, *88*(24), 2285–2293. https://doi.org/10.1212/wnl.0000000000004035

Hoh, B. L., Chapman, P. H., Loeffler, J. S., Carter, B. S., & Ogilvy, C. S. (2002). Results of multimodality treatment for 141 patients with brain arteriovenous malformations and seizures: Factors associated with seizure incidence and seizure outcomes. *Neurosurgery*, *51*(2), 303–309 discussion 309–311.

Howard, G. M., Radloff, M., & Sevier, T. L. (2004). Epilepsy and sports participation. *Current Sports Medicine Reports*, *3*(1), 15–19. https://doi.org/10.1249/00149619-200402000-00004

Jiao, Y., Wu, J., Chen, X., Li, Z., Ma, J., Cao, Y., & Wang, S. (2019). Spetzler-Martin grade IV and V arteriovenous malformations: Treatment outcomes and risk factors for negative outcomes after surgical resection. *Journal of Clinical Neuroscience*, *61*, 166–173. https://doi.org/10.1016/j.jocn.2018.10.101

Jo, H. J., Kenney-Jung, D. L., Balzekas, I., Welker, K. M., Jones, D. T., Croarkin, P. E., Benarroch, E. E., & Worrell, G. A. (2019). Relationship between seizure frequency and functional abnormalities in limbic network of medial temporal lobe epilepsy. *Frontiers in Neurology*, *10*, 488. https://doi.org/10.3389/fneur.2019.00488

Jobst, B. C., & Cascino, G. D. (2017). Thalamus as a "hub" to predict outcome after epilepsy surgery. *Neurology*, *88*(24), 2246–2247. https://doi.org/10.1212/wnl.0000000000004043

Kang, J. Y., & Mintzer, S. (2016). Driving and epilepsy: A review of important issues. *Current Neurology and Neuroscience Reports*, *16*(9), 80. https://doi.org/10.1007/s11910-016-0677-y

Khambhati, A. N., Davis, K. A., Oommen, B. S., Chen, S. H., Lucas, T. H., Litt, B., & Bassett, D. S. (2015). Dynamic network drivers of seizure generation, propagation and termination in human neocortical epilepsy. *PLoS Computational Biology*, *11*(12), e1004608. https://doi.org/10.1371/journal.pcbi.1004608

Lawton, M. T., Rutledge, W. C., Kim, H., Stapf, C., Whitehead, K. J., Li, D. Y., Krings, T., terBrugge, K., Kondziolka, D., Morgan, M. K., Moon, K., & Spetzler, R. F. (2015). Brain arteriovenous malformations. *Nature Reviews. Disease Primers*, *1*, 15008. https://doi.org/10.1038/nrdp.2015.8

Liu, S., Li, A., Liu, Y., Li, J., Wang, M., Sun, Y., Qin, W., Yu, C., Jiang, T., & Liu, B. (2020). MIR137 polygenic risk is associated with schizophrenia and affects functional connectivity of the dorsolateral prefrontal cortex. *Psychological Medicine*, *50*(9), 1510–1518. https://doi.org/10.1017/S0033291719001442

Liu, Z., Wang, Y., Liu, X., Du, Y., Tang, Z., Wang, K., Wei, J., Dong, D., Zang, Y., Dai, J., Jiang, T., & Tian, J. (2018). Radiomics analysis allows for precise prediction of epilepsy in patients with low-grade gliomas. *NeuroImage: Clinical*, *19*, 271–278. https://doi.org/10.1016/j.nicl.2018.04.024

Luo, C., Xia, Y., Li, Q., Xue, K., Lai, Y., Gong, Q., Zhou, D., & Yao, D. (2011). Diffusion and volumetry abnormalities in subcortical nuclei of patients with absence seizures. *Epilepsia*, *52*(6), 1092–1099. https://doi.org/10.1111/j.1528-1167.2011.03045.x

Mansouri, A. M., Germann, J., Boutet, A., Elias, G. J. B., Mithani, K., Chow, C. T., Karmur, B., Ibrahim, G. M., McAndrews, M. P., Lozano, A. M., Zadeh, G., & Valiante, T. A. (2020). Identification of neural networks preferentially engaged by epileptogenic mass lesions through lesion network mapping analysis. *Scientific Reports*, *10*(1), 10989. https://doi.org/10.1038/s41598-020-67626-x

Mohan, A., Roberto, A. J., Mohan, A., Lorenzo, A., Jones, K., Carney, M. J., Liogier-Weyback, L., Hwang, S., & Lapidus, K. A. (2016). The significance of the default mode network (DMN) in neurological and neuropsychiatric disorders: A review. *The Yale Journal of Biology and Medicine*, *89*(1), 49–57.

Nelissen, N., Van Paesschen, W., Baete, K., Van Laere, K., Palmini, A., Van Billoen, H., & Dupont, P. (2006). Correlations of interictal FDG-PET metabolism and ictal SPECT perfusion changes in human temporal lobe epilepsy with hippocampal sclerosis. *NeuroImage*, *32*(2), 684–695. https://doi.org/10.1016/j.neuroimage.2006.04.185

Riley, J. D., Moore, S., Cramer, S. C., & Lin, J. J. (2011). Caudate atrophy and impaired frontostriatal connections are linked to executive dysfunction in temporal lobe epilepsy. *Epilepsy & Behavior*, *21*(1), 80–87. https://doi.org/10.1016/j.yebeh.2011.03.013

Schramm, J. (2017). Seizures associated with cerebral arteriovenous malformations. *Handbook of Clinical Neurology*, *143*, 31–40. https://doi.org/10.1016/B978-0-444-63640-9.00004-7

Seabold S, & Perktold J. (2010). *Statsmodels: Econometric and statistical modeling with python*. Proceedings of the 9th Python in Science Conference, 92–96. https://doi.org/10.25080/Majora-92bf1922-011

Snider, S. B., Hsu, J., Darby, R. R., Cooke, D., Fischer, D., Cohen, A. L., Grafman, J. H., & Fox, M. D. (2020). Cortical lesions causing loss of consciousness are anticorrelated with the dorsal brainstem. *Human Brain Mapping*, *41*(6), 1520–1531. https://doi.org/10.1002/hbm.24892

Soldozy, S., Norat, P., Yağmurlu, K., Sokolowski, J. D., Sharifi, K. A., Tvrdik, P., Park, M. S., & Kalani, M. Y. S. (2020). Arteriovenous malformation presenting with epilepsy: A multimodal approach to diagnosis and treatment. *Neurosurgical Focus*, *48*(4), E17. https://doi.org/10.3171/2020.1.Focus19899

Sun, Y., Tian, R. F., Li, A. M., Liu, X. G., Chen, J., & Shi, H. (2016). Unruptured epileptogenic brain arteriovenous malformations. *Turkish Neurosurgery*, *26*(3), 341–346. https://doi.org/10.5137/1019-5149.JTN.9190-13.1

Thurman, D. J., Beghi, E., Begley, C. E., Berg, A. T., Buchhalter, J. R., Ding, D., Hesdorffer, D. C., Hauser, W. A., Kazis, L., Kobau, R., Kroner, B., Labiner, D., Liow, K., Logroscino, G., Medina, M. T., Newton, C. R., Parko, K., Paschal, A., Preux, P. M., … Wiebe, S. (2011). Standards for epidemiologic studies and surveillance of epilepsy. *Epilepsia*, *52*(Suppl 7), 2–26. https://doi.org/10.1111/j.1528-1167.2011.03121.x

Virtanen, P., Gommers, R., Oliphant, T. E., Haberland, M., Reddy, T., Cournapeau, D., Burovski, E., Peterson, P., Weckesser, W., Bright, J., van der Walt, S. J., Brett, M., Wilson, J., Millman, K. J., Mayorov, N., Nelson, A. R. J., Jones, E., Kern, R., Larson, E., … van Mulbregt, P. (2020). SciPy 1.0: Fundamental algorithms for scientific computing in Python. *Nature Methods*, *17*(3), 261–272. https://doi.org/10.1038/s41592-019-0686-2

Wang, Y., Fan, X., Zhang, C., Zhang, T., Peng, X., Li, S., Wang, L., Ma, J., & Jiang, T. (2014). Anatomical specificity of O6-methylguanine DNA methyltransferase protein expression in glioblastomas. *Journal of Neuro-Oncology*, *120*(2), 331–337. https://doi.org/10.1007/s11060-014-1555-6

Wang, Y., Qian, T., You, G., Peng, X., Chen, C., You, Y., Yao, K., Wu, C., Ma, J., Sha, Z., Wang, S., & Jiang, T. (2015). Localizing seizure-susceptible brain regions associated with low-grade gliomas using voxel-based lesion-symptom mapping. *Neuro-Oncology*, *17*(2), 282–288. https://doi.org/10.1093/neuonc/nou130

Wei, H. L., An, J., Zeng, L. L., Shen, H., Qiu, S. J., & Hu, D. W. (2015). Altered functional connectivity among default, attention, and control networks in idiopathic generalized epilepsy. *Epilepsy & Behavior*, *46*, 118–125. https://doi.org/10.1016/j.yebeh.2015.03.031

Whelan, C. D., Altmann, A., Botia, J. A., Jahanshad, N., Hibar, D. P., Absil, J., Alhusaini, S., Alvim, M. K. M., Auvinen, P., Bartolini, E., Bergo, F. P. G., Bernardes, T., Blackmon, K., Braga, B., Caligiuri, M. E., Calvo, A., Carr, S. J., Chen, J., Chen, S., … Sisodiya, S. M. (2018). Structural brain abnormalities in the common epilepsies assessed in a worldwide ENIGMA study. *Brain*, *141*(2), 391–408. https://doi.org/10.1093/brain/awx341

Zhang, Y., Yan, P., Liang, F., Ma, C., Liang, S., & Jiang, C. (2019). Predictors of epilepsy presentation in unruptured brain arteriovenous malformations: A quantitative evaluation of location and radiomics features on T2-weighted imaging. *World Neurosurgery*, *125*, e1008–e1015. https://doi.org/10.1016/j.wneu.2019.01.229

SUPPORTING INFORMATION

Additional supporting information can be found online in the Supporting Information section at the end of this article.

TABLE S1 Detailed demographics of the patients

TABLE S2 Prevalence of seizures among the three risk categories

FIGURE S1 The conjunction analyses results for the 40%-threshold scheme. The conjunction analyses for the 40% threshold scheme indicated that connectivity (positive in red and negative in blue) to the left caudate and precuneus was both sensitive and specific for lesions causing seizures.

Transparent Science Questionnaire for Authors

How to cite this article: Zhao, S.-Z., Zhao, Y.-X., Liao, X.-H., Huo, R., Li, H., Jiao, Y.-M., Weng, J.-C., Wang, J., Liu, B., & Cao, Y. (2023). Unruptured brain arteriovenous malformations causing seizures localize to one common brain network. *Journal of Neuroscience Research*, *101*, 245–255. https://doi.org/10.1002/jnr.25142